Hindawi Publishing Corporation
Journal of Nanomaterials
Volume 2012, Article ID 365062, 7 pages
doi:10.1155/2012/365062

Research Article

An Electrically Conductive and Organic Solvent Vapors Detecting Composite Composed of an Entangled Network of Carbon Nanotubes Embedded in Polystyrene

R. Olejnik,[1,2] P. Slobodian,[1,2] P. Riha,[3] and P. Saha[1,2]

[1] *Polymer Centre, Faculty of Technology, Tomas Bata University in Zlin, 76001 Zlin, Czech Republic*
[2] *Centre of Polymer Systems, University Institute, Tomas Bata University in Zlin, Nad Ovcirnou 3685, 76001 Zlin, Czech Republic*
[3] *Institute of Hydrodynamics, Academy of Sciences, 16612 Prague, Czech Republic*

Correspondence should be addressed to P. Slobodian, slobodian@ft.utb.cz

Received 30 January 2012; Accepted 12 March 2012

Academic Editor: Sevan P. Davtyan

A composite composed of electrically conductive entangled carbon nanotubes embedded in a polystyrene base has been prepared by the innovative procedure, when the nonwoven polystyrene filter membrane is enmeshed with carbon nanotubes. Both constituents are then interlocked by compression molding. The mechanical and electrical resistance testing show that the polymer increases nanotube network mechanical integrity, tensile strength, and the reversibility of electrical resistance in deformation cycles. Another obvious effect of the supporting polymer is the reduction of resistance temperature dependence of composite and the reproducibility of methanol vapor sensing.

1. Introduction

Recent technology progress relies heavily on the use of materials that provide advanced structural and functional capabilities. In this respect, entangled carbon nanotube (CNT) network of buckypaper presents great promise for developing high-performance polymeric materials [1–3]. The networks can proportionally transfer their unique properties into composites and bring substantial improvements in structural strength, electrical and thermal conductivity, electromagnetic interference shielding, and so forth compared to polymer composites with carbon nanotube particulate filler.

The first polymer composite with CNT network was fabricated via filtering nanotube dispersion through fine filtration mesh [4]. Nanotubes stuck to each other and formed a thin entangled structure of pure nanotubes, later dubbed buckypaper. The network was then fixed by a polymer solution (epoxy [5, 6] or bismaleimide resin [1], polyvinyl alcohol, polyvinylpyrrolidone and polyethylene oxide water solutions [7]) to form composites.

However, the fabrication of CNT network-based polymer composite described above was rather laborious. Our idea is to circumvent polymer solution methods and to suggest a simple and easier manufacturing of multiwall carbon nanotube (MWNT) network-based polymer composites. The novel process consists in using nonwoven polystyrene (PS) filter as an integrating and supporting element on which nanotubes cumulate and form a network during MWNT suspension filtration. The nanotubes slightly infiltrate into the filter and adhere to it, finally forming a continuous layer. The obtained MWNT/PS-layered composite is compression molded above the melting temperature of PS, which causes transformation of the filter into flexible PS film. Repeating layering of MWNT/PS films enables producing bulky material.

The processing technique seems promising for continuous manufacturing of CNT networks/polymer composites since the filter support ensures the composite compactness. Peeling off MWNT layer from the membrane, which is common in previous methods, is eliminated here as well as network impregnation by polymer solutions.

In the present paper, the scanning electron microscopy (SEM) of a layered structure of MWNT network/polystyrene composite is carried out together with the tests of composite

tensile deformation and electrical resistance. The additional testing reveals the effect of the supporting polymer on the resistance temperature dependence of composite and the reproducibility of methanol vapor sensing.

2. Materials

Purified MWCNTs produced by chemical vapor deposition of acetylene which were supplied by Sun Nanotech Co. Ltd., China. According to the supplier, the nanotube diameter is 10–30 nm, length 1–10 μm, with a purity of ~90% and (volume) resistivity of 0.12 Ωcm. Further details on the nanotubes were obtained by means of the transmission electron microscopy (TEM) analysis presented in our previous paper [8]. From the corresponding micrographs, the diameter of individual nanotubes was determined to be between 10 and 60 nm, their length from tenths of micron up to 3 μm. The maximum aspect ratio of the measured nanotubes is thus about 300. The multiwall consists of about 15–35 rolled layers of graphene. Another analyses estimate oxygen content on CNT surface 5.5 at percentage with O/C ratio 0.06 measured by X-ray photoelectron spectroscopy, the high thermal stability measured by Thermogravimetric Analysis when only negligible degradation in the range of temperatures up to 700°C occurs, that is, a loss of mass ca 3 wt. % [9].

Polystyrene is a commercial polymer (Krasten 137, Kaucuk-Unipetrol Group, M_n = 102 530, and M_w/M_n = 2.75). Sodium dodecyl sulfate (SDS) and 1-pentanol were used as surfactant and cosurfactant, respectively. Methyl isobutyl ketone (MIBK) and dimethylformamide (DMF) were used as PS solvents, and tetraethylammonium bromide was used to adjust conductivity of PS solutions for electrospinning (filter preparation).

3. Experimental

MWNTs were used for the preparation of aqueous paste: 1.6 g of nanotubes and ~50 mL of deionized water were mixed with the help of a mortar and pestle. The paste was diluted in deionized water with SDS and 1-pentanol [10–12]. Then NaOH/water solution was added to adjust pH to the value of 10 [13]. The final nanotube concentration in the dispersion was 0.3 wt. % concentration of SDS and 1-pentanol 0.1 M and 0.14 M, respectively [10]. The dispersion was sonicated in Dr. Hielscher GmbH apparatus (ultrasonic horn S7, amplitude 88 μm, power density 300 W/cm^2, and frequency 24 kHz) under the temperature of ca 50°C for 2 hours.

Polystyrene nonwoven mats for filtration of nanotube dispersion were prepared by electrospinning from PS solution. The polymer was dissolved in a mixture of MIBK/DMF with the volume ratio 3 : 1 and PS concentration 15 wt. %. Electrical conductivity of the solution was adjusted to 75 μS/cm by tetraethylammonium bromide. PS nanofiber layer was manufactured using the NanoSpider (Elmarco, s.r.o.) equipped with a steel rotating electrode with needles and a steel cylindrical collecting electrode (more details in [14]). Electrospinning was carried out under the following conditions: electric voltage 75 kV (Matsusada DC power supply), temperature 20–25°C, relative humidity 25–35%, and the electrode rotation speed 8 min^{-1}. The motion rate of antistatic polypropylene nonwoven fabric which collects nanofibers was 0.16 m/min. To produce final PS nonwoven filters, the prepared nanofiber porous layer (thickness of about 1 mm) was subjected to hot pressing under 0.6 MPa and temperature 80°C.

In order to prepare entangled MWNT network on the supporting PS filter, a vacuum-filtration method was used. The formed disk-shaped network was washed several times by deionized water (to reach neutral pH) and methanol in situ. Subsequently, MWNT network with PS filter was placed between two acetone moistened filter papers and dried between two iron plates at room temperature for 24 hours. The final drying continued without iron plates at 40°C for another day. The thickness of the nonwoven PS filter was typically 0.5–0.8 mm, and the thickness of MWNT entangled network, according of the amount of dispersion filtered, was from 0.02 to 0.26 mm. The formed PS filter-supported MWNT network was then compression molded at 190°C. Thus, the originally porous PS filter was transformed into a film.

For comparison, pure carbon nanotube networks were prepared by filtration of dispersions through polyurethane nonwoven filters prepared again by electrospinning according to procedure described in [14]. After filtration, the MWNT sediment was washed by deionized water and methanol in situ and drained between dry filter papers for a moment before the entangled MWNT sediment was gently peeled off the filter and dried.

The structure of PS nonwoven filter as well as that of MWNT network was investigated with a scanning electron microscope (SEM) Vega LMU (Tescan s.r.o., Czech Republic). The sample was deposited on carbon targets and covered with a thin Au/Pd layer. The observation was carried out in the regime of secondary electrons.

The strength of the network was measured in a simple test. The sample materials (PS filter-supported MWNT network; pure entangled MWNT network) were cut into stripes (length 45 mm and width 10 mm) and stretched stepwise with 60 sec delay in deformation reading in each step.

To measure the dependence of electrical resistance on tensile deformation of MWNT/PS composite, the stripe (length 30 mm and width 5 mm) cut from the prepared MWNT/PS composite was fixed on PS tensile test specimen (dog bone shape) using 20 wt. % solution of PS in butanone. Two electrical contacts were fixed to the stripe by silver colloid electroconductive paint Dotite D-550 (SPI Supplies). The electrical resistance was measured lengthwise during 7 consecutive tensile cycles by a two-point technique with multimeter Sefram 7338.

MWNT/PS composite as a potential resistive gas sensor for organic vapor detection was identified by the electrical resistance measurement in a chemical vapor atmosphere. The resistance of network stripe cut out from the manufactured disks (length 15 mm, width 5 mm, and thickness

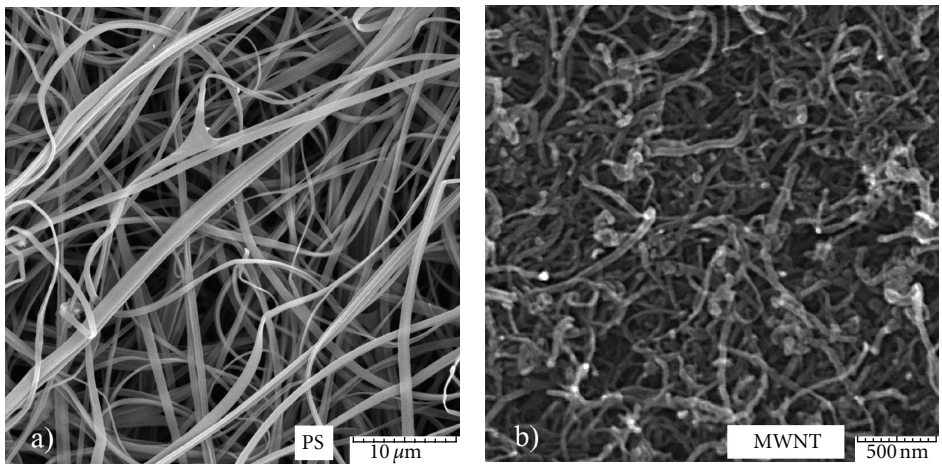

(a) (b)

Figure 1: SEM image of (a) PS filter prepared by electrospinning (displayed scaler 10 μm) and (b) surface of entangled MWNT network (scaler 500 nm).

ca 0.3 mm) was measured along the specimen length by the two-point technique using multimeter Sefram 7338. The stripe was placed on a planar holder with Cu electrodes fixed on both sides of the specimen. Time-dependent electrical resistance measurement was performed during adsorption and desorption cycles. In the former case the holder with the specimen was quickly transferred into an airtight conical flask full of methanol vapor, a layer of which was at the bottom. The measurement was conducted in the saturated vapor at atmospheric pressure, temperature 25°C and relative humidity 60%. After 6 minutes of measurement the holder was promptly removed from the flask, and for the next 6 minutes the sample was measured in the mode of desorption. This was repeated five times in consecutive cycles.

The temperature dependence of electrical resistance of MWNT networks and MWNT/PS composites were measured by a four-point method according to van der Pauw's idea [15]. The apparatuses used in the set up were Keithley K7002 scanner, Keithley K7011-S switching card, programmable current source Keithley K2410, Keithley K6517 electrometer and PC with GPIB cec488 and AD25PCI SE transducer cards and SVOR25TER connector. The resistance was measured at constant current 0.01 A in the course of heating from −40°C to 150°C (step 10°C) using thermostatic bath (Haake).

4. Results

4.1. SEM Results. The surface of PS filter prepared by technology of electrospinning and the upper surface of the MWNT network accumulated on the filter are shown as SEM micrographs in Figures 1(a) and 1(b), respectively. PS fibers are straight with smooth surface, submicron sizes with the average diameter of 0.6 ± 0.3 μm. The pores between them have an average size of about 0.5 μm. The apparent density of PS filter is $\rho_{\text{filter}} = 0.1\,\text{g/cm}^3$, thus its porosity ϕ for the measured PS density $\rho_{\text{PS}} = 1.04\,\text{g/cm}^3$ was calculated (from the relation below) to be about 0.9. The pores allow partial infiltration of MWNT into the filter at the beginning of filtration. When the pores are filled with nanotubes, the filter cake (pure nanotube entangled network) is formed above the filter surface, as shown in Figure 2.

The porosity of MWNT network was calculated to be $\phi = 0.67$ from relation $\phi = 1 - \rho_{\text{net}}/\rho_{\text{MWNT}}$, where $\rho_{\text{net}} = 0.56 \pm 0.03\,\text{g/cm}^3$ denotes the measured apparent density of the nanotube network ($n = 10$), and $\rho_{\text{MWNT}} = 1.7\,\text{g/cm}^3$ is the measured average density of nanotubes ($n = 3$). This density is very close to the theoretical value for MWNT, which is $1.8\,\text{g/cm}^3$ [16]. Also the network porosity corresponds to the published values for MWNT networks [17].

MWNT network was firmly embedded in PS filter by compression molding. The temperature of processing was 190°C, which is well above the glass transition temperature of PS used for experiments (T_g = 92°C, determined by differential scanning calorimetry technique). The melting phase was followed by cooling below PS glass transition temperature, when both layers were firmly linked.

Figure 3 shows composite arrangement after compression molding. The thickness of MWNT network was proportional to the volume of filtered MWNT dispersion and was typically from 26 μm to 260 μm. The arrangement of the layers of nanotube networks and PS is arbitrary. For instance, the structure prepared by double-sided filtration, MWNT-PS-MWNT composite, is shown in Figure 3(c). Other layer arrangements can be prepared by overlaying several MWNT/PS composite units prior to compression molding.

The role of MWCNT network thickness, that is, MWCNT, concentration in the conductive MWCNT network/PS composite, is not determining as in the case of particulate MWCNT/polymer composites. Though there is certainly an optimal and/or limiting MWCNT network thickness constituting resistive characteristics of the conductive

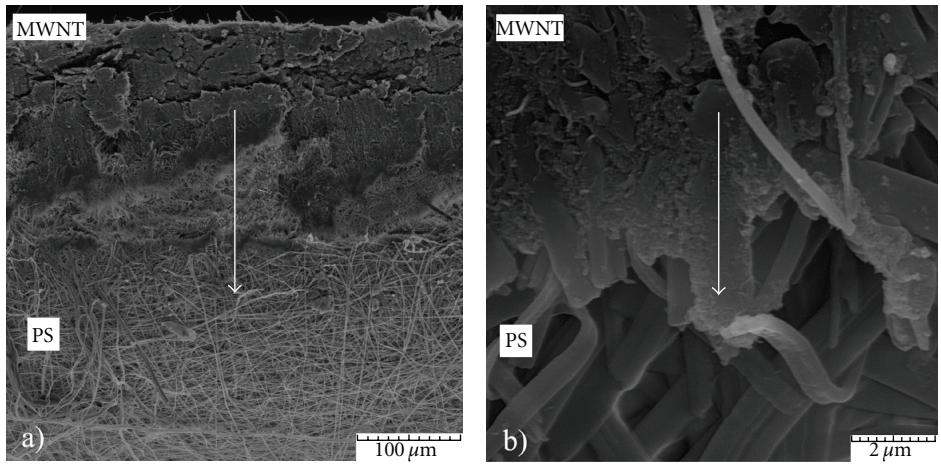

(a) (b)

Figure 2: (a) cross-section of composite consisting of MWNT network (upper part) and PS filter (lower part) before compression molding (scaler 100 μm). (b) the arrow indicates nanotube infiltration illustrated in detail in the enlarged image (scaler 2 μm).

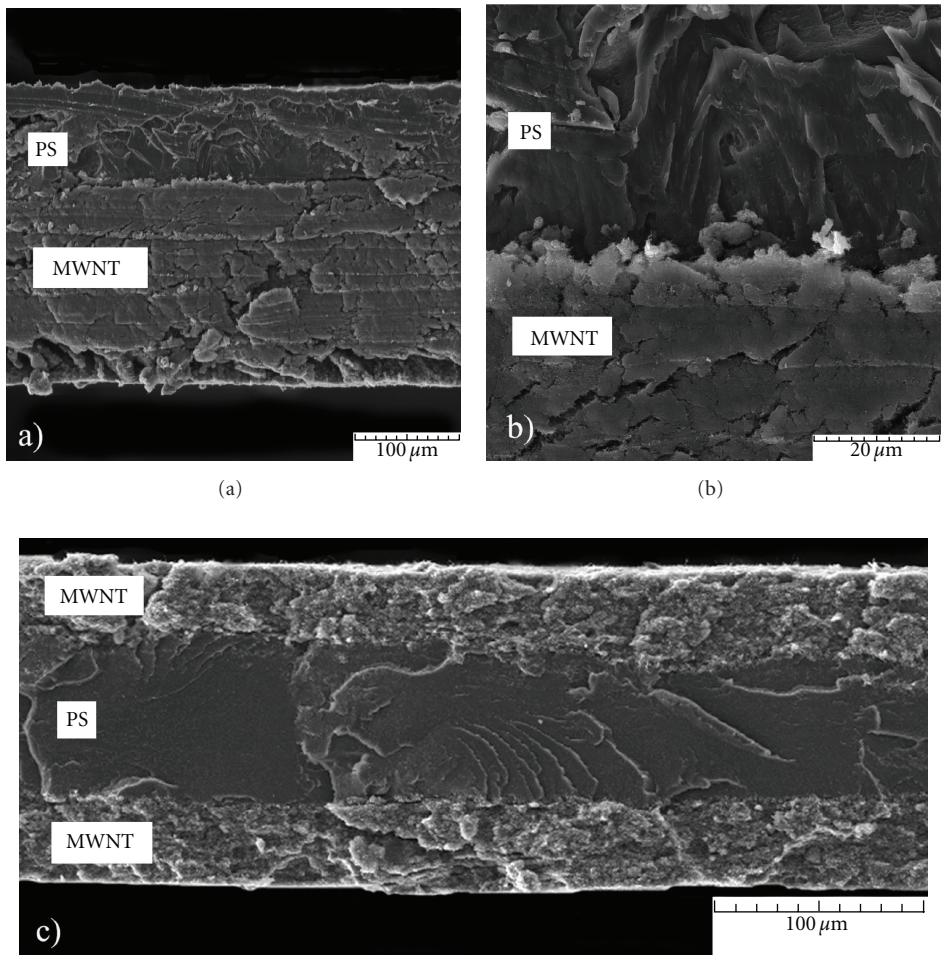

(a) (b)

(c)

Figure 3: SEM micrographs of layered MWNT network/PS composite after compression molding. (a) PS film (thicknesses about 80 μm) with attached nanotube network (260 μm) (scaler 100 μm), (b) the interface between nanotube network and PS film (scaler 20 μm), and (c) MWNT-PS-MWNT layer arrangement to decrease composite resistance (scaler 100 μm).

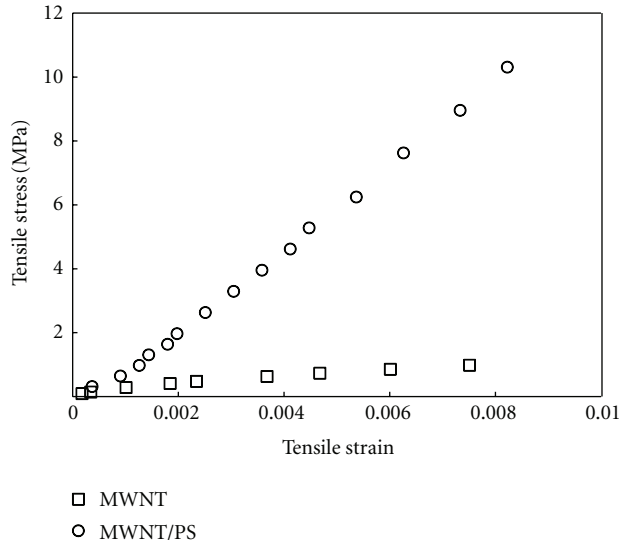

Figure 4: Tensile properties of MWNT network/PS composite (circles) and MWNT network (squares) in tensile test. Thickness of MWNT network is about 120 μm and MWNT/PS composite about 200 μm.

composite, this aspect is not investigated in this paper. Some informative results about this issue can be found in our paper [18].

To examine the length, thickness and multiwall arrangement of MWNT, TEM analysis was used. The obtained values slightly differ from the properties declared by the manufacturer. From TEM micrographs the diameter of individual nanotubes was determined to be between 10 and 60 nm, their length from tenth of micron up to 3 μm; the maximum aspect ratio is thus about 300. The number of coaxially rolled layers of graphene was typically from 10 till 35 with the interlayer distance of about 0.35 nm [8, 18].

4.2. Tensile Test Results. The results of tensile testing of MWNT network and PS filter supported MWNT network are shown in Figure 4. The measured stress/strain dependence for pure MWNT network indicates the tensile modulus of about 600 MPa and the ultimate tensile strength ~1 MPa. The values are relatively low, which corresponds to short nanotubes used for the research. PS filter support has a positive effect on the tensile strength of MWNT/PS composite, as can be seen in the same figure. The determined tensile modulus is about 1300 MPa and the ultimate tensile strength 10.3 MPa.

The electrical resistance change of MWNT network/PS composite is monitored by a two-point technique in extension/relaxation cycles. The results are shown in Figure 5 as the strain dependence of the relative resistance change $(R - R_0)/R_0$ due to the increasing tensile stress indicated in the figure. R and R_0 denote the measured and the initial resistance before the first extension/relaxation cycle, respectively. The resistance mechanism is apparently not reversible in the initial cycle, since the relaxation curve has a residual resistance increase in the offload state (Figure 6).

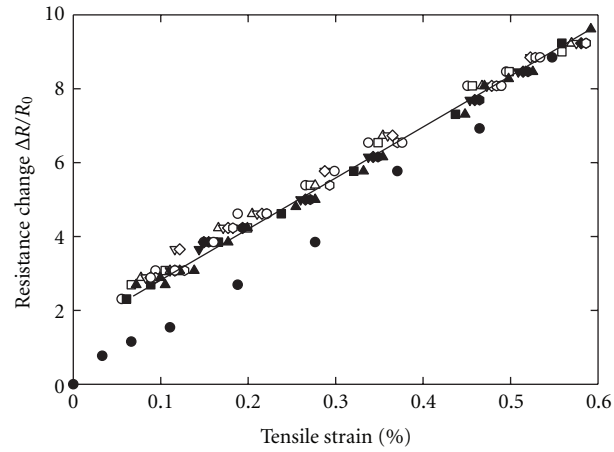

Figure 5: Relative change of electrical resistance versus tensile stress for MWNT network/PS composite subjected to 7 successive elongation/relaxation cycles (network thickness is about 20 μm; the filled and open symbols denote the extension part and the relaxation part of cycles, resp.). The solid circles represent the extension part of the first cycle and the full line the linear fitting of resistance change in subsequent cycles. The strain increase corresponds to the step increase of tensile stress 0.8, 1.9, 2.8, 4.3, 6.4, 9.2, 10.3, and 11.8 MPa, respectively.

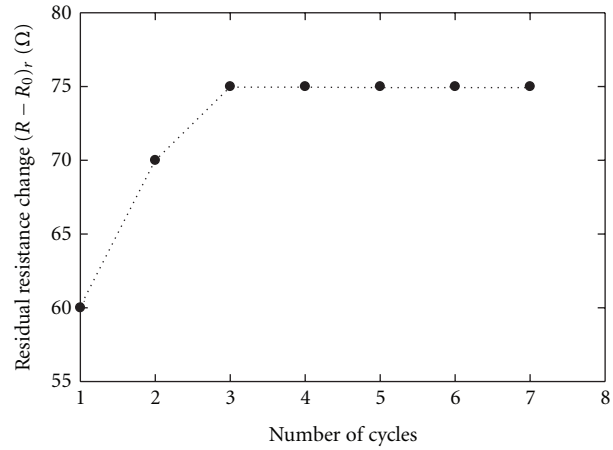

Figure 6: Residual resistance change versus number of cycles for MWNT network/PS composite subjected to 7 successive elongation/relaxation cycles.

Nevertheless, the ongoing extension cycles have a stabilizing effect on the resistance-elongation loops, and the normalized resistance change is fitted in Figure 5 by a linear dependence on tensile strain. The residual resistance change $(R - R_0)$, defined as the residual minimum resistance change during each cycle, tends to reach immediately to an asymptotic value (Figure 6). It indicates that during first deformations the nanotube network gets the structure which stays more or less the same regardless the number of deformation cycles. This mechanical stabilization is favorable for the use of the composite as a sensing element of elongation, especially when the network is suitably deformed in advance.

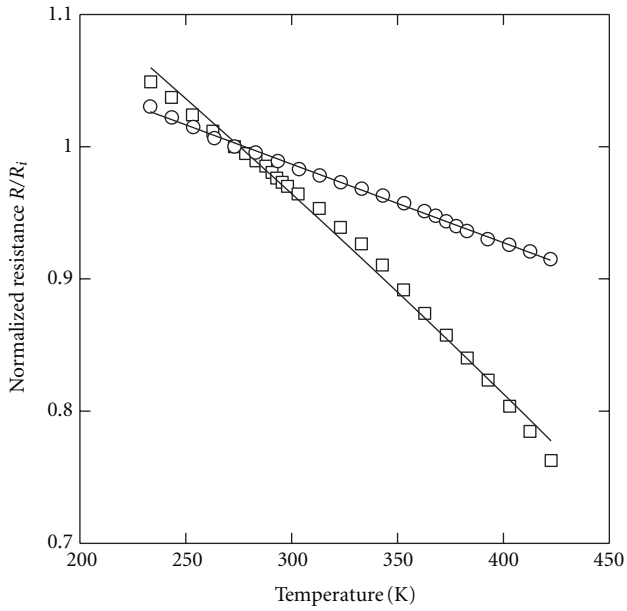

Figure 7: Temperature-dependent normalized resistance of MWNT network/PS composite (circles) and MWNT network (squares). The solid lines represent description by (1).

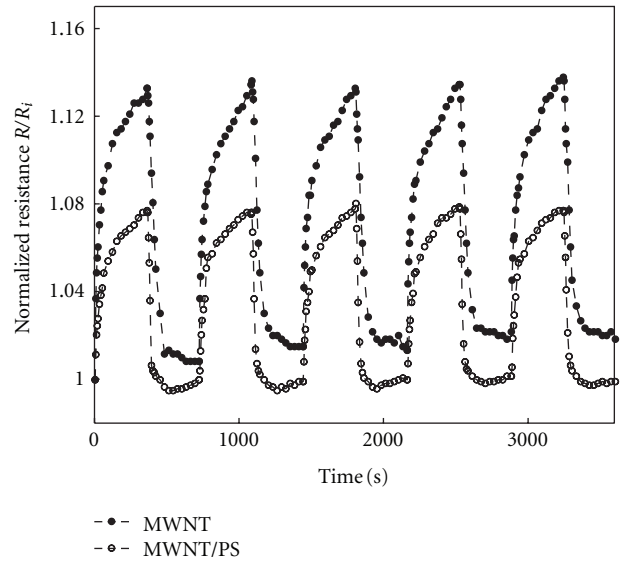

Figure 8: Time-dependent normalized resistance of MWNT network/PS composite (open circles) and MWNT network (filled circles) repeatedly exposed to methanol vapors at room temperature. The length of cycles of exposure and desorption is 360 sec.

The mechanism of resistance change during elongation combines probably a decrease of local contact forces between nanotubes as well as reduction of number of contacts. The decrease of contact forces restrains a contact of nanotubes, which in turn leads to the increase of contact resistance between crossing nanotubes. Besides that the extension straightens the nanotubes what may result in less contacts between them. Since the contact points act as parallel resistors, their decreasing number causes an enhancement of MWNT network resistance.

4.3. Electrical Resistance: the Effect of Temperature and Chemical Vapor. The effect of temperature and chemical vapor on the electrical resistance was also tested, and the results are presented in Figures 7 and 8, respectively. Figure 7 demonstrates that both the composite and pure MWNT network exhibit nonmetallic behavior ($d(R/R_i)/dT < 0$) over the investigated temperature range from 230 to 420 K. The negative slope indicates the presence of tunneling barriers, which dominate resistive behavior of the tested materials. The best description of the data presented in Figure 7 is obtained by the series heterogeneous model when the resistance is described as the sum of metallic (MWNT are regarded as metallic conductors) and barrier portions of the conduction path [19–22]:

$$\frac{R}{R_i} = aT + b\exp\left[\frac{c}{(T+d)}\right], \tag{1}$$

where a means the temperature coefficient arising from metallic resistance, and the second term (hopping/tunneling term) represents fluctuation-induced tunneling through barriers between metallic regions. T denotes temperature, b is constant depending on the geometrical factors from the effective fraction of the length for the barrier portion, and c; d are constants depending on the barrier to conduction parameters [19–22].

An obvious effect of the supporting polymer is a reduction of the temperature dependence of resistance. The resistance ratio R_{230}/R_{420} (values at the corresponding temperatures) is reduced from 1.35 in the case of MWNT network to 1.12 in the composite case.

The affinity of MWNT network with and without PS filter support to chemical vapor at room temperature is demonstrated in Figure 8. Results of repeated exposure to methanol vapors reveal that both materials response has good reproducibility. As stated in [9, 23], there are two possible mechanisms in which vapors can reversibly interact with nanotubes: physisorption, which does not involve charge transfer and chemisorption, which does. The short response time of the two materials to exposure to methanol and subsequent recovery suggests a physisorption mechanism. Methanol molecules could be absorbed to nanotube surface, which may cause a change in metallic/barrier conduction proportion resulting in the increase of resistance.

5. Concluding Remarks

Several techniques were applied to investigate a new type of composite: PS filter-supported entangled multiwall carbon nanotube network. The SEM observation indicates the penetration of carbon nanotubes into the nonwoven polystyrene filtering membrane and their tight bonding after the compression molding. The mechanical testing reveals the effect of elongation on the composite electrical resistance when a repeated stretching is exerted. The measurements have shown fivefold resistance increase at the maximum

strain as well as stability and linearity of resistance change. The sensitivity of the composite to an organic solvent vapor (methanol) has been investigated also by a resistance measurement. The resistance variation as a response to physisorption and desorption of a vapor during cycles was found to be reversible and reproducible. Thus, the testing indicates a good potentiality of the composite composed of electrically conductive entangled carbon nanotube network embedded in a polystyrene base to be applied as a sensing element for tensile deformation and organic vapors.

Acknowledgments

The work was supported by the Operational Program of Research and Development for Innovations cofunded by the European Regional Development Fund (ERDF), the National budget of Czech Republic within the framework of the Centre of Polymer Systems project (Reg. no.: CZ.1.05/2.1.00/03.0111), the Czech Ministry of Education, Youth and Sports project (MSM 7088352101). This paper was also supported by the internal grant of TBU in Zlín no. IGA/FT/2012/022 funded from the resources of specific university research and by the Fund of Institute of Hydrodynamics AV0Z20600510.

References

[1] Q. Cheng, J. Bao, J. Park, Z. Liang, C. Zhang, and B. Wang, "High mechanical performance composite conductor: multi-walled carbon nanotube sheet/bismaleimide nanocomposites," *Advanced Functional Materials*, vol. 19, no. 20, pp. 3219–3225, 2009.

[2] D. Wang, P. Song, C. Liu, W. Wu, and S. Fan, "Highly oriented carbon nanotube papers made of aligned carbon nanotubes," *Nanotechnology*, vol. 19, no. 7, Article ID 075609, 2008.

[3] S. Wang, Z. Liang, B. Wang, and C. Zhang, "High-strength and multifunctional macroscopic fabric of single-walled carbon nanotubes," *Advanced Materials*, vol. 19, no. 9, pp. 1257–1261, 2007.

[4] D. A. Walters, M. J. Casavant, X. C. Qin et al., "In-plane-aligned membranes of carbon nanotubes," *Chemical Physics Letters*, vol. 338, no. 1, pp. 14–20, 2001.

[5] J. Gou, "Single-walled nanotube bucky paper and nanocomposite," *Polymer International*, vol. 55, no. 11, pp. 1283–1288, 2006.

[6] Z. Wang, Z. Liang, B. Wang, C. Zhang, and L. Kramer, "Processing and property investigation of single-walled carbon nanotube (SWNT) buckypaper/epoxy resin matrix nanocomposites," *Composites A*, vol. 35, no. 10, pp. 1225–1232, 2004.

[7] G. Xu, Q. Zhang, W. Zhou, J. Huang, and F. Wei, "The feasibility of producing MWCNT paper and strong MWCNT film from VACNT array," *Applied Physics A*, vol. 92, no. 3, pp. 531–539, 2008.

[8] P. Slobodian, P. Riha, A. Lengalova, and P. Saha, "Compressive stress-electrical conductivity characteristics of multiwall carbon nanotube networks," *Journal of Materials Science*, vol. 46, no. 9, pp. 3186–3190, 2011.

[9] P. Slobodian, P. Riha, A. Lengalova, P. Svoboda, and P. Saha, "Multi-wall carbon nanotube networks as potential resistive gas sensors for organic vapor detection," *Carbon*, vol. 49, no. 7, pp. 2499–2507, 2011.

[10] C. S. Chern and L. J. Wu, "Microemulsion polymerization of styrene stabilized by sodium dodecyl sulfate and short-chain alcohols," *Journal of Polymer Science A*, vol. 39, no. 19, pp. 3199–3210, 2001.

[11] A. S. Patole, S. P. Patole, J. B. Yoo, J. H. Ahn, and T. H. Kim, "Effective in situ synthesis and characteristics of polystyrene nanoparticle-Covered multiwall carbon nanotube composite," *Journal of Polymer Science B*, vol. 47, no. 15, pp. 1523–1529, 2009.

[12] A. S. Patole, S. P. Patole, S. Y. Jung, J. B. Yoo, J. H. An, and T. H. Kim, "Self assembled grapheme/carbon nanotube/polystyrene hybrid nanocomposite by in situ microemulsion polymerization," *European Polymer Journal*, vol. 48, pp. 252–259, 2012.

[13] H. T. Ham, Y. S. Choi, and I. J. Chung, "An explanation of dispersion states of single-walled carbon nanotubes in solvents and aqueous surfactant solutions using solubility parameters," *Journal of Colloid and Interface Science*, vol. 286, no. 1, pp. 216–223, 2005.

[14] D. Kimmer, P. Slobodian, D. Petras, M. Zatloukal, R. Olejnik, and P. Saha, "Polyurethane/MWCNT nanowebs prepared by electrospinning process," *Journal of Applied Polymer Science*, vol. 111, pp. 2711–2714, 2009.

[15] L. J. van der Pauw, "A method of measuring specific resistivity and Hall effect of discs of arbitrary shape," *Philips Research Reports*, vol. 13, pp. 1–9, 1958.

[16] X. L. Xie, Y. W. Mai, and X. P. Zhou, "Dispersion and alignment of carbon nanotubes in polymer matrix: a review," *Materials Science and Engineering R*, vol. 49, no. 4, pp. 89–112, 2005.

[17] R. L. D. Whitby, T. Fukuda, T. Maekawa, S. L. James, and S. V. Mikhalovsky, "Geometric control and tuneable pore size distribution of buckypaper and buckydiscs," *Carbon*, vol. 46, no. 6, pp. 949–956, 2008.

[18] P. Slobodian, P. Riha, A. Lengalova, R. Olejnik, and P. Saha, "Effect of compressive strain on electric resistance of multi-wall carbon nanotube networks," *Journal of Experimental Nanoscience*, vol. 6, pp. 294–304, 2011.

[19] A. Allaoui, S. V. Hoa, P. Evesque, and J. Bai, "Electronic transport in carbon nanotube tangles under compression: the role of contact resistance," *Scripta Materialia*, vol. 61, no. 6, pp. 628–631, 2009.

[20] A. B. Kaiser, Y. W. Park, G. T. Kim, E. S. Choi, G. Düsberg, and S. Roth, "Electronic transport in carbon nanotube ropes and mats," *Synthetic Metals*, vol. 103, no. 1–3, pp. 2547–2550, 1999.

[21] M. Shiraishi and M. Ata, "Conduction mechanisms in single-walled carbon nanotubes," *Synthetic Metals*, vol. 128, no. 3, pp. 235–239, 2002.

[22] S. Kulesza, P. Szroeder, J. K. Patyk, J. Szatkowski, and M. Kozanecki, "High-temperature electrical transport properties of buckypapers composed of doped single-walled carbon nanotubes," *Carbon*, vol. 44, no. 11, pp. 2178–2183, 2006.

[23] S. G. Wang, Q. Zhang, D. J. Yang, P. J. Sellin, and G. F. Zhong, "Multi-walled carbon nanotube-based gas sensors for NH_3 detection," *Diamond and Related Materials*, vol. 13, no. 4–8, pp. 1327–1332, 2004.